From $^1_\infty[(UO_2)_2O(MoO_4)_4]^{6-}$ to $^1_\infty[(UO_2)_2(MoO_4)_3(MoO_5)]^{6-}$ infinite chains in $A_6U_2Mo_4O_{21}$ (A=Na, K, Rb, Cs) compounds: Synthesis and crystal structure of $Cs_6[(UO_2)_2(MoO_4)_3(MoO_5)]$

S. Yagoubi [a,b], S. Obbade [c,*], S. Saad [a], F. Abraham [a]

[a] Unité de Catalyse et de Chimie du Solide, UCCS UMR CNRS 8181, USTL, ENSCL-B.P. 90108, 59652 Villeneuve d'Ascq Cedex, France
[b] Groupe de Radiochimie, Institut de Physique Nucléaire d'Orsay, Université Paris-Sud XI, 91406 Orsay Cedex, France
[c] Laboratoire d'Électrochimie et de Physicochimie des Matériaux et des Interfaces, LEPMI, UMR 5279, CNRS-Grenoble INP-UdS-UJF,
1130 Rue de la Piscine, BP 75, 38402 Saint-Martin d'Hères, France

ARTICLE INFO

ABSTRACT

A new caesium uranyl molybdate belonging to the $M_6U_2Mo_4O_{21}$ family has been synthesized by solid-state reaction and its structure determined from single-crystal X-ray diffraction data. Contrary to the other alkali uranyl molybdates of this family (A=Na, K, Rb) where molybdenum atoms adopt only tetrahedral coordination and which can be formulated $A_6[(UO_2)_2O(MoO_4)_4]$, the caesium compound $Cs_6U_2Mo_4O_{21}$ should be written $Cs_6[(UO_2)_2(MoO_4)_3(MoO_5)]$ with molybdenum atoms in tetrahedral and square pyramidal environments. $Cs_6[(UO_2)_2(MoO_4)_3(MoO_5)]$ crystallizes in the triclinic symmetry with space group $P\bar{1}$ and a=10.4275(14) Å, b=15.075(2) Å, c=17.806(2) Å, α=70.72(1)°, β=80.38(1)° and γ=86.39(1)°, V=2604.7(6) Å³, Z=4, ρ_{mes}=5.02(2) g/cm³ and ρ_{cal}=5.08(3) g/cm³. A full-matrix least-squares refinement on the basis of F^2 yielded R_1=0.0464 and wR_2=0.0950 for 596 parameters with 6964 independent reflections with $I \geq 2\sigma(I)$ collected on a BRUKER AXS diffractometer with Mo($K\alpha$) radiation and a CCD detector. The crystal structure of Cs compound is characterized by $^1_\infty[(UO_2)_2(MoO_4)_3(MoO_5)]^{6-}$ parallels chains built from U_2O_{13} dimeric units, MoO_4 tetrahedra and MoO_5 square pyramids, whereas, Na, K and Rb compounds are characterized by $^1_\infty[(UO_2)_2O(MoO_4)_4]^{6-}$ parallel chains formulated simply of U_2O_{13} units and MoO_4 tetrahedra.

Infrared spectroscopy measurements using powdered samples synthesized by solid-state reaction, confirm the structural results. The thermal stability and the electrical conductivity are also studied. The four compounds decompose at low temperature (between 540 and 610 °C).

1. Introduction

Since the first oil crisis, uranium, the only natural element having a fissile isotope (U235), plays an important part in the field of the energy production in the world, particularly in France. Thus, any progress in physical and chemical knowledge of this element, can present in the short or medium term an interest for the control of different problems of the manufacture, the storage and the reprocessing of nuclear fuel. So, the materials resulting from the association of ions uranyl UO_2^{2+} and oxoanions $X_mO_n^{p-}$, with X=C, N, P, S, Si, As, I, transition metals etc., have had a very intense research activity in these last decades [1,2]. This research is motivated not only by the environmental aspects, like the possible oxidation of the uranium during the storage, the

formation of the new compounds in the contaminated grounds and the evolution of the obtained products after the nuclear waste deterioration, but also by cationic exchanges, ionic conductivity and fluorescence properties, that these materials can generate [3–17]. From a solid-state chemistry point view, the uranyl ion association to different oxoanions is particularly interesting because it frequently generates original structures: two-dimensional structures (2D) by the formation of infinite layers, or more scarcely three-dimensional (3D) frameworks presenting infinite tunnels [18]. These structures favour the mobility of the cations localized in the tunnels or between layers, as well as the possibility of intercalation/desintercalation of these cations.

Considering the presence of the long-living radioactive fission isotopes ^{137}Cs and [93]Mo in consequent quantities in radioactive waste and spent nuclear fuel, and the possibility of the chemical interaction, in normal or accidental conditions, of both fission products (^{137}Cs and [93]Mo) between them as well as with uranium oxide to form different caesium uranyl molybdate compounds,

* Corresponding author.
E-mail addresses: said.obbade@phelma.grenoble-inp.fr,
said.obbade@lepmi.grenoble-inp.fr (S. Obbade).

the identification of such compounds likely to form is necessary. Thus, the Cs_2O–MoO_3–UO_3 ternary system has been extensively studied these three last decades, and several new caesium uranyl molybdates have been identified and their crystal structures determined [19–29]. The reaction between the three metals Cs–U–Mo in alteration products of spent nuclear fuel, to form caesium uranyl molybdate compounds, under the similar conditions with those expected in the nuclear waste repository at Yucca Mountain site in Nevada, has been already shown by Buck et al. [10]. This study revealed the presence of orthorhombic mixed Cs/Ba uranyl molybdate $(Cs_{0.8}Ba_{0.6})[(UO_2)_5(MoO_4)O_4(OH)_6](\sim 6H_2O)$, characterized by Analytical Transmission Electron Microscopy, after corrosion of commercial oxide spent nuclear fuel. Thus, additional investigations of this ternary system are very important for the understanding of evolution and alteration of spent nuclear fuel and radioactive waste.

So, if one considers the ternary system A_2O–MoO_3–UO_3 where A corresponds to monovalent cations (Li^+, Na^+, K^+, Rb^+, Cs^+, Ag^+, Tl^+ and NH_4^+), several uranyl molybdates families have been evidenced and their crystal structures determined from X-ray diffraction data [10,19–46]. Concerning caesium uranyl molybdates, only eight compounds have been reported and their crystal structures were determined using single crystal X-ray diffraction data. According to their composition the uranyl molybdate entities adopt various dimensionalities in agreement with the diagram proposed by Alekseev et al. [29]: $Cs_6[(UO_2)(MoO_4)_4]$ contains $[UO_2(MoO_4)_4]^{4-}$ units (0D) [24], $Cs_2[(UO_2)O(MoO_4)$ is based upon chains of UO_6 and MoO_4 polyhedra (1D) [29], the β-form of $Cs_2[(UO_2)_2(MoO_4)_3]$ [25], $Cs_2[(UO_2)(MoO_4)_2]$ and its monohydrate $Cs_2[(UO_2)(MoO_4)_2](H_2O)$ [22,26] are layered compounds (2D), the layers being built of UO_6 and MoO_4 entities, in $Cs_4[(UO_2)_3O(MoO_4)_2(MoO_5)]$ the layers are built from both MoO_4 and $MoO5$ polyhedra [24], finally the α-form of $Cs_2[(UO_2)_2(MoO_4)_3]$ [25] and the dihydrate $Cs_2[(UO_2)_6(MoO_4)_7(H_2O)_2]$ [23,34] are framework-based structures (3D). Some of these compounds have been also evidenced and characterized with other A^+ monovalent cations.

The present work is dedicated to the crystal structure determination of a new Cs-uranyl molybdate $Cs_6[(UO_2)_2(MoO_4)_3(MoO_5)]$ synthesized by solid-state reaction. Its crystal structure was determined from single crystal X-ray diffraction data and compared to those of the other compounds $A_6[(UO_2)_2O(MoO_4)_4]$ (A=Na, K and Rb) previously reported [45,46]. The thermal, electrical and spectroscopic results of this alkaline uranyl molybdate family are also reported

2. Experimental

2.1. Synthesis of single crystals and powder samples

Yellow-orange transparent single crystals were obtained by solid-state reactions from mixtures of U_3O_8 (Prolabo, 1 mol) and MoO_3 (Prolabo, 3 mol) and an excess of Cs_2CO_3 (Aldrich, 10 mol). The mixture was slowly heated in platinum crucibles up to 950 °C, maintained at this temperature during 12 h and then cooled at 5 °C/h to room temperature. The molten mixture was washed with hot water and ethanol to dissolve alkaline salt excess and separate yellow-orange single crystals of $Cs_6U_2Mo_4O_{21}$. Presence and proportions of the metal elements, Cs, U and Mo, in different obtained crystals were confirmed by Energy Dispersive Spectroscopy analysis performed using a JEOL JSM-5300 Scanning Microscope equipped with IMIX system of Princeton Gamma Technology (PGT).

Pure polycrystalline samples of $A_6U_2Mo_4O_{21}$ (A=Na, K, Rb, Cs) were prepared by conventional solid-state reactions, using pure initial materials U_3O_8, MoO_3 and A_2CO_3 taken in molar ratio of 2:12:9 according to the following reaction:

$$2/3U_3O_8 + 4MoO_3 + 3A_2CO_3 + 1/3O_2(air) \rightarrow A_6U_2Mo_4O_{21} + 3CO_2$$
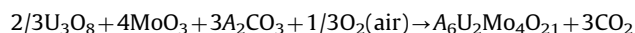
The homogeneous mixtures were slowly heated up to 500 °C in a platinum crucible and maintained at this temperature during 10 days, with intermediate grindings, and finally slowly cooled to

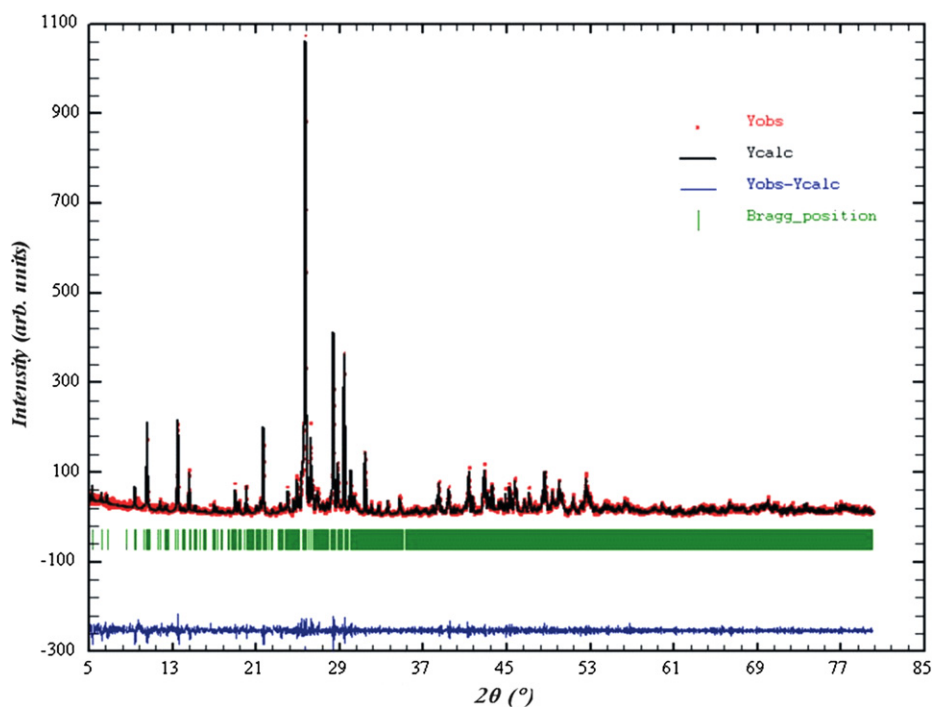**Fig. 1.** Observed (dots), calculated (solid line) powder X-ray diffraction profiles of $Cs_6[(UO_2)_2(MoO_4)_3(MoO_5)]$. Difference ($Y_{obs} - Y_{cal}$) appears at the bottom of the plot and allowed reflections are indicated by vertical lines.

room temperature. For each sample, the reaction progress is controlled by powder X-ray diffraction. Unit cell parameters of $Cs_6U_2Mo_4O_{21}$ were refined by using powder X-ray diffraction data collected with a Bruker D8 θ/θ diffractometer equipped by CuKα radiation, using Bragg–Brentano geometry, with steps of 0.03° and a counting time of 20 s per step, within an angular range of 10–80° in 2θ. The unit cell parameters were refined using Rietveld method [47,48]. The refinement was carried out using the "*pattern matching*" option of Fullprof program [49], where only the profile parameters (cell dimensions, peak shapes, background, zero point correction and symmetry) have been refined. The peak shape was described by a pseudo-Voigt function with an asymmetry correction at low angles. In order to describe the angular dependence of the peak full-width at half-maximum (H), the formulation of Caglioti et al. [50] was used: $H^2 = U\tan^2\theta + V\tan\theta + W$ where U, V and W parameters were refined in the process. For $Cs_6U_2Mo_4O_{21}$, the cell parameters refinement led to the following values $a=10.4216(3)$ Å, $b=15.0702(4)$ Å, $c=17.7967(5)$ Å, $\alpha=70.73(1)°$, $\beta=80.39(2)°$ and $\gamma=86.39(2)$ with the following profile factors: $R_p=0.035$, $R_{wp}=0.046$ and $\chi^2=1.05$. The good agreement between observed and calculated powder X-ray diffraction diagrams is shown in Fig. 1 and the indexed powder pattern is reported in the Table 1. The reliability of the unit cell refinement and indexing reflections is indicated by the conventional figures of merit F_{20}, defined by Smith and Snyder [51], $F_{20}=48$ (0.0032, 130). The density measured with an automated Micromeritics Accupy 1330 helium pycnometer using a 1-cm^3 cell, indicates a good agreement between the calculated and measured densities, with four

formula per unit cell ($\rho_{mes}=5.02(2)$ g/cm^3, $\rho_{cal}=5.08(3)$ g/cm^3) for $Cs_6U_2Mo_4O_{21}$.

2.2. Thermal analyses, electrical conductivity and infrared spectroscopy measurements

To determine the thermal stability of the studied compounds, Differential Thermal Analyses (DTA) were performed in air, using SETARAM 92-1600 thermal analyzer in the temperature range of 20–900 °C with heating and cooling rate 1.5 °C/min using platinum crucibles.

To evidence alkaline cations mobility in the four compounds $A_6U_2Mo_4O_{21}$ ($A=$Na, K, Rb and Cs), electrical conductivity measurements were carried out on cylindrical pellets (diameter, 5 mm; thickness, 3.5 mm), obtained using a conventional cold press and sintered at 500 °C for 2 days, followed by slow cooling, (5 °C/h), down to room temperature. Gold electrodes were vacuum-deposited on both flat surfaces of the pellets. Conductivity measurements were performed by ac impedance spectroscopy over the range of 1–10^6 Hz with a Solartron 1170 frequency-response analyzer. Measurements were performed with 20 °C intervals between 200 and 500 °C on both heating and cooling. Each set of values was recorded after a 1 h stabilization time at a given temperature.

For each compound infrared spectrum was recorded using the KBr dispersion technique (1 mg of sample dispersed in 125 mg of KBr and pressed at the pressure of 150 bars) with a Bruker Vector 22 Fourier Transform Infrared Spectrometer, which covers the range of 400–4000 cm^{-1} with a resolution of 0.1 cm^{-1}.

Table 1
Observed and calculated X-ray powder diffraction pattern for $Cs_6[(UO_2)_2(MoO_4)_3(MoO_5)]$.

h	k	l	2θ obs	2θ cal	I (%)	h	k	l	2θ obs	2θ cal	I (%)
0	0	1	5.3350	5.3279	4	−2	−3	3	34.7204	34.7214	5
0	1	0	6.2250	6.2149	3	1	−2	6	38.4082	38.4096	8
0	1	1	6.7570	6.7459	2	4	3	1	38.4595	38.4607	9
1	0	1	9.4140	9.3962	5	1	−4	4	38.5783	38.5784	2
1	1	0	10.5710	10.5768	22	1	6	5	38.7943	38.7943	2
0	2	1	11.8312	11.8359	2	3	5	1	39.4020	39.4022	7
0	2	2	13.5034	13.5080	24	−3	2	5	39.9124	39.9121	3
−1	1	2	14.5966	14.6011	10	0	6	6	41.3052	41.3044	8
1	0	3	16.9980	16.9800	4	−4	2	3	41.3770	41.3753	10
2	−1	1	18.9850	18.9890	8	−4	−3	1	41.7373	41.7375	5
−2	1	1	19.3507	19.3542	3	1	7	4	42.8292	42.8277	12
−1	2	3	20.0590	20.0624	7	−2	3	7	43.2340	43.2334	6
1	3	3	21.0315	21.0256	2	1	−6	2	43.5627	43.5606	8
0	0	4	21.4030	21.4067	4	−1	7	1	44.2157	44.2127	4
2	0	3	21.6960	21.7000	33	−2	0	7	44.4690	44.4688	5
−2	2	2	23.3390	23.3408	3	−3	−4	3	44.8286	44.8276	7
2	−1	3	24.0459	24.0496	7	−5	0	1	45.2730	45.2718	9
1	−1	4	24.5841	24.5878	4	1	7	0	45.3890	45.3863	4
−2	1	3	24.9152	24.9179	10	4	−4	2	45.7460	45.7444	9
2	−3	0	25.6604	25.6623	100	4	1	7	46.6232	46.6247	4
−1	3	4	26.2162	26.2184	24	2	3	9	47.0841	47.0853	7
3	1	2	26.4193	26.4228	7	−4	5	1	47.6247	47.6217	3
0	0	5	26.8427	26.8461	6	0	−5	5	48.3970	48.3951	5
0	−4	1	27.2808	27.2824	3	0	7	7	48.5962	48.5939	10
−3	1	1	27.7513	27.7534	4	2	−3	7	49.3220	49.3213	6
3	−1	2	28.1570	28.1595	5	−5	−3	1	49.9657	49.9643	9
2	4	2	28.3838	28.3862	48	5	4	5	50.2649	50.2652	6
3	2	3	28.7931	28.7966	14	2	8	2	51.2848	51.2814	5
−2	2	4	29.4370	29.4387	41	5	5	4	52.0370	52.0364	4
0	5	1	30.0540	30.0766	11	3	7	7	52.5282	52.5270	9
0	−4	2	30.3699	30.3710	5	4	−3	6	52.8865	52.8851	5
0	5	0	31.4225	31.4229	17	−5	−4	1	53.1574	53.1553	3
−2	4	3	32.0610	32.0610	4	−4	4	6	53.4591	53.4553	3
2	4	5	32.7124	32.7149	3	5	5	6	54.3262	54.3259	4
−3	−2	2	33.6010	33.6022	4						

2.3. Single crystal X-ray diffraction and structure determination of $Cs_6U_2Mo_4O_{21}$

For structure determination, a well-shaped yellow-orange single crystal of $Cs_6U_2Mo_4O_{21}$ phase was selected, mounted on fibreglass and aligned on a Bruker AXS X-ray diffractometer equipped with a 1K SMART CCD. Intensities were collected at room temperature using $MoK\alpha$ ($\lambda=0.71073$ Å) radiation selected by a graphite monochromator. The individual frames were measured using a ω-scan technique with an omega rotation of 0.3° and an acquisition time of 30 s per frame. A total of 1800 frames were collected covering the full sphere. After data collection, the intensity data were integrated and corrected for Lorentz-polarization and background effects using the Bruker program SAINT [52]. Once the data processing was performed, the absorption corrections were computed using a semi-empirical method based on redundancy with the SADABS program [53]. Details of the data collection and refinement are given in Table 2. The triclinic unit-cell parameters of $Cs_6U_2Mo_4O_{21}$ single crystal were refined to $a=10.4275(14)$ Å, $b=15.075(2)$ Å, $c=17.806(2)$ Å, $\alpha=70.72(1)°$, $\beta=80.38(1)°$ and $\gamma=86.39(1)°$.

Crystal structure was determined in the centrosymmetric P-1 space group, by direct methods using SHELXS program [54] which readily localize the more heavy atoms U and Cs. The positions of molybdenum and oxygen atoms were deduced from subsequent refinements and difference Fourier maps, using the SHELXL option of the SHELXTL software [55]. The atomic scattering factors for neutral atoms were taken from "International Tables for X-ray Crystallography" [56]. The last cycle of refinement including atomic positions and anisotropic displacement parameters for all atoms, yielded to the final refinement factor $R1=0.046$ for 6964 independent reflections. Refinement results

Table 2
Crystal data, intensity collection and structure refinement parameters for $Cs_6(UO_2)_2(MoO_4)_3(MoO_5)$.

Compound	$Cs_6(UO_2)_2(MoO_4)_3(MoO_5)$
Crystal data	
Crystal symmetry	Triclinic
Space group	$\bar{P}$-1
Unit cell	$a=10.4275(14)$ Å
	$b=15.075(2)$ Å
	$c=17.806(2)$ Å
	$\alpha=70.72(1)°$
	$\beta=80.38(1)°$
	$\gamma=86.39(1)°$
	$V=2604.7(6)$ Å^3
Z	4
Calculated density	$\rho_{cal}=5.08(3)$ g/cm^3
Measured density	$\rho_{mes}=5.02(2)$ g/cm^3
Data collection	
Temperature (K)	293(2)
Radiation Mo($K\alpha$)	0.71073 Å
Scan mode	ω
Recording angular range (deg.)	3.24/29.27
Recording reciprocal space	$-14 \leq h \leq 14$
	$-19 \leq k \leq 20$
	$-23 \leq h \leq 23$
Number of reflections measured/independent	12,635/6964
Absorption μ (cm^{-1})	225.98
Colour	Yellow
Refinement	
Refined parameters/restraints	596/0
Goodness of fit on F^2	1.012
R1 [$I > 2\sigma(I)$]	0.046
wR2 [$I > 2\sigma(I)$]	0.095
Largest diff peak and hole (e Å^{-3})	2.457/−3.290

Table 3
Atomic coordinates and equivalent displacement parameters (Å^2) for $Cs_6(UO_2)_2(MoO_4)_3(MoO_5)$.

Atom	Site	x	y	z	U_{eq}
U1	2i	0.39897(6)	0.09439(5)	0.17648(4)	0.0150(2)
U2	2i	0.81701(6)	−0.29846(5)	0.02682(4)	0.0156(2)
U3	2i	−0.31502(6)	0.78861(5)	0.47221(4)	0.0145(2)
U4	2i	0.10827(6)	0.41416(5)	0.32271(4)	0.0153(2)
Cs1	2i	0.46569(11)	−0.13847(9)	0.07678(8)	0.0258(3)
Cs2	2i	0.01619(12)	0.20235(8)	0.22275(7)	0.0254(3)
Cs3	2i	0.04102(11)	0.63218(9)	0.42322(8)	0.0251(3)
Cs4	2i	−0.28975(12)	0.60956(9)	0.33049(8)	0.0275(3)
Cs5	2i	0.76763(12)	−0.11934(9)	0.18420(8)	0.0313(3)
Cs6	2i	1.19262(13)	−0.47557(9)	0.04663(8)	0.0318(3)
Cs7	2i	0.50538(11)	0.29636(8)	0.26608(7)	0.0242(3)
Cs8	2i	0.44331(13)	−0.42008(10)	0.19485(8)	0.0344(3)
Cs9	2i	−0.69057(11)	0.67709(9)	0.55717(8)	0.0284(3)
Cs10	2i	0.05619(12)	−0.09147(9)	0.31000(8)	0.0315(3)
Cs11	2i	0.20803(12)	−0.17653(10)	−0.05987(8)	0.0351(4)
Cs12	2i	0.33759(13)	−0.00814(10)	0.43866(9)	0.0340(3)
Mo1	2i	0.14704(15)	0.03107(11)	0.06651(10)	0.0182(4)
Mo2	2i	−0.01324(15)	0.85061(11)	0.55222(10)	0.0185(4)
Mo3	2i	0.41713(14)	−0.18384(11)	0.32005(10)	0.0163(4)
Mo4	2i	−0.32771(14)	0.55176(11)	0.56648(9)	0.0157(3)
Mo5	2i	0.45587(14)	0.32033(11)	0.04850(9)	0.0175(4)
Mo6	2i	−0.30693(15)	0.05541(11)	0.31619(10)	0.0174(4)
Mo7	2i	0.07522(14)	0.68746(11)	0.17702(10)	0.0166(4)
Mo8	2i	0.83050(15)	−0.56170(11)	0.18417(10)	0.0175(4)
O1	2i	0.9222(12)	−0.3273(8)	−0.0534(7)	0.027(3)
O2	2i	0.2873(11)	0.1333(8)	0.2484(7)	0.023(2)
O3	2i	−0.1749(11)	0.0393(8)	0.2490(8)	0.026(3)
O4	2i	−0.0291(12)	0.4454(9)	0.3864(7)	0.027(3)
O5	2i	−0.2022(12)	0.7788(9)	0.3876(7)	0.030(3)
O6	2i	0.5149(10)	0.2218(8)	0.1340(7)	0.018(2)
O7	2i	−0.2322(11)	0.4913(8)	0.6506(7)	0.022(3)
O8	2i	0.5127(12)	0.0470(9)	0.1109(7)	0.026(3)
O9	2i	0.2397(11)	0.3825(9)	0.2568(8)	0.027(3)
O10	2i	−0.4302(12)	0.8081(9)	0.5531(7)	0.027(3)
O11	2i	0.2783(12)	−0.2488(8)	0.3647(8)	0.028(3)
O12	2i	0.3441(11)	0.3837(8)	−0.0240(7)	0.019(3)
O13	2i	0.7182(11)	−0.2681(9)	0.1088(8)	0.031(3)
O14	2i	0.3723(11)	−0.0671(9)	0.2688(7)	0.028(3)
O15	2i	−0.2229(11)	0.6595(8)	0.5658(7)	0.021(3)
O16	2i	−0.2800(11)	0.1553(9)	0.3398(8)	0.028(3)
O17	2i	0.2207(12)	0.745(1)	0.1526(8)	0.034(4)
O18	2i	−0.0299(12)	0.7263(10)	0.2469(8)	0.038(4)
O19	2i	0.5984(11)	0.3271(8)	−0.0204(7)	0.024(3)
O20	2i	0.0098(12)	0.7052(9)	0.0871(7)	0.028(3)
O21	2i	−0.4480(12)	0.0707(9)	0.2694(8)	0.032(3)
O22	2i	−0.3311(13)	−0.0414(8)	0.4057(7)	0.029(3)
O23	2i	−0.3967(11)	0.6529(8)	0.4874(7)	0.022(3)
O24	2i	0.2224(12)	0.0229(9)	0.1499(8)	0.035(4)
O25	2i	0.8679(12)	−0.4558(9)	0.1042(8)	0.032(3)
O26	2i	−0.0228(12)	0.7408(8)	0.6284(8)	0.029(3)
O27	2i	0.0905(12)	0.1485(9)	0.0295(8)	0.037(4)
O28	2i	0.6994(13)	−0.5463(10)	0.2520(8)	0.036(4)
O29	2i	−0.4768(13)	0.5124(10)	0.6227(8)	0.040(4)
O30	2i	0.5122(12)	−0.2334(10)	0.2539(7)	0.032(3)
O31	2i	0.0184(12)	−0.0443(9)	0.0988(8)	0.037(4)
O32	2i	0.1282(11)	0.8525(9)	0.4837(8)	0.033(4)
O33	2i	0.1053(14)	0.5635(9)	0.2179(8)	0.033(3)
O34	2i	0.5094(12)	−0.181(1)	0.3943(9)	0.041(4)
O35	2i	0.2568(14)	0.0033(11)	−0.0057(9)	0.049(4)
O36	2i	−0.1498(12)	0.8618(9)	0.5045(8)	0.031(3)
O37	2i	0.4509(13)	0.4052(9)	0.0955(8)	0.032(3)
O38	2i	0.9672(13)	−0.5978(8)	0.2337(8)	0.033(4)
O39	2i	−0.2644(13)	0.4878(9)	0.5035(8)	0.036(4)
O40	2i	−0.0120(13)	0.9378(9)	0.5955(8)	0.036(4)
O41	2i	0.7909(12)	−0.649(1)	0.1474(8)	0.032(4)
O42	2i	0.3266(11)	0.2154(8)	0.0654(7)	0.023(3)

of the atomic coordinates with equivalent isotropic thermal factors are reported in Table 3 and anisotropic displacement parameters are listed in Table 4. Table 5 provides the most

Table 4
Anisotropic displacement parameters (Å^2) for $Cs_6(UO_2)_2(MoO_4)_3(MoO_5)$.

Atom	U11	U22	U33	U12	U13	U23
U1	0.0145(3)	0.0154(4)	0.0149(4)	0.0005(3)	−0.0027(3)	−0.0045(3)
U2	0.0172(3)	0.0154(4)	0.0146(4)	0.0000(3)	−0.0031(3)	−0.0049(3)
U3	0.0153(3)	0.0143(3)	0.0130(4)	−0.0001(3)	−0.0027(3)	−0.0032(3)
U4	0.0154(3)	0.0154(4)	0.0149(4)	0.0000(3)	−0.0029(3)	−0.0042(3)
Cs1	0.0270(6)	0.0254(7)	0.0245(7)	−0.0012(5)	−0.0043(5)	−0.0072(5)
Cs2	0.0300(6)	0.0240(7)	0.0215(7)	0.0009(5)	−0.0056(5)	−0.0060(5)
Cs3	0.0240(6)	0.0233(7)	0.0267(7)	0.0031(5)	−0.0041(5)	−0.0068(5)
Cs4	0.0302(6)	0.0271(7)	0.0268(7)	−0.0056(5)	−0.0031(5)	−0.0105(6)
Cs5	0.0294(7)	0.0316(7)	0.0352(8)	−0.0069(6)	−0.0048(6)	−0.0126(6)
Cs6	0.0378(7)	0.0276(7)	0.0362(8)	0.0004(6)	−0.0052(6)	−0.0190(6)
Cs7	0.0272(6)	0.0238(6)	0.0231(7)	0.0033(5)	−0.0072(5)	−0.0085(5)
Cs8	0.0305(7)	0.0364(8)	0.0275(8)	−0.0008(6)	−0.0063(6)	0.0022(6)
Cs9	0.0272(7)	0.0290(7)	0.0276(8)	−0.0014(6)	−0.0060(5)	−0.0061(6)
Cs10	0.0265(6)	0.0302(7)	0.0316(8)	0.0000(6)	−0.0062(5)	−0.0008(6)
Cs11	0.0229(6)	0.0394(8)	0.0345(9)	0.0000(6)	−0.0039(6)	−0.0011(7)
Cs12	0.0367(7)	0.0342(8)	0.0371(8)	−0.0020(6)	−0.0013(6)	−0.0214(6)
Mo1	0.0164(7)	0.0176(8)	0.0186(9)	0.0002(6)	−0.0031(6)	−0.0032(7)
Mo2	0.0190(8)	0.0187(8)	0.0180(8)	−0.0008(7)	−0.0063(6)	−0.0045(7)
Mo3	0.0164(7)	0.0162(8)	0.0155(9)	−0.0009(6)	−0.0039(6)	−0.0031(6)
Mo4	0.0154(7)	0.0154(8)	0.0158(8)	−0.0010(6)	−0.0027(6)	−0.0041(6)
Mo5	0.0179(8)	0.0179(8)	0.0156(9)	−0.0006(6)	−0.0033(6)	−0.0035(6)
Mo6	0.0179(8)	0.0158(8)	0.0182(9)	−0.0015(6)	−0.0052(6)	−0.0036(7)
Mo7	0.0160(7)	0.0164(8)	0.0163(9)	−0.0005(6)	−0.0039(6)	−0.0032(7)
Mo8	0.0201(8)	0.0152(8)	0.0178(9)	−0.0018(6)	−0.0047(6)	−0.0051(7)
O1	0.035(7)	0.020(7)	0.019(7)	0.012(6)	0.000(6)	−0.003(6)
O2	0.027(7)	0.033(8)	0.003(6)	0.009(6)	0.002(5)	−0.001(5)
O3	0.026(7)	0.023(7)	0.027(8)	−0.001(6)	0.003(6)	−0.008(6)
O4	0.029(7)	0.031(8)	0.024(8)	0.004(6)	−0.001(6)	−0.015(6)
O5	0.040(8)	0.040(9)	0.012(7)	−0.011(7)	0.005(6)	−0.014(6)
O6	0.018(6)	0.020(7)	0.014(7)	−0.006(5)	0.004(5)	−0.006(5)
O7	0.026(7)	0.011(6)	0.028(8)	−0.011(5)	−0.009(6)	0.000(5)
O8	0.031(7)	0.031(8)	0.021(8)	0.006(6)	−0.005(6)	−0.018(6)
O9	0.020(6)	0.030(8)	0.035(8)	0.017(6)	−0.005(6)	−0.018(6)
O10	0.036(7)	0.033(8)	0.011(7)	0.002(6)	0.006(6)	−0.012(6)
O11	0.039(8)	0.014(7)	0.028(8)	−0.013(6)	−0.002(6)	−0.004(6)
O12	0.023(6)	0.021(7)	0.015(7)	−0.002(5)	−0.012(5)	−0.003(5)
O13	0.024(7)	0.033(8)	0.032(9)	−0.010(6)	0.012(6)	−0.010(7)
O14	0.025(7)	0.029(8)	0.024(8)	0.001(6)	−0.015(6)	0.007(6)
O15	0.026(7)	0.018(7)	0.027(8)	−0.012(5)	−0.011(6)	−0.012(6)
O16	0.024(7)	0.022(7)	0.045(9)	0.006(6)	−0.013(6)	−0.016(7)
O17	0.025(7)	0.037(9)	0.044(10)	0.002(6)	−0.011(6)	−0.018(7)
O18	0.030(8)	0.05(1)	0.034(9)	0.005(7)	0.007(6)	−0.021(7)
O19	0.023(7)	0.022(7)	0.024(8)	0.003(5)	−0.005(5)	−0.006(6)
O20	0.037(8)	0.024(7)	0.021(8)	−0.002(6)	−0.008(6)	−0.005(6)
O21	0.035(8)	0.030(8)	0.022(8)	−0.006(6)	−0.007(6)	0.006(6)
O22	0.047(8)	0.019(7)	0.020(8)	0.013(6)	−0.021(6)	−0.001(6)
O23	0.020(6)	0.019(7)	0.027(8)	−0.001(5)	−0.012(5)	−0.003(6)
O24	0.029(7)	0.037(9)	0.036(9)	−0.020(6)	−0.009(6)	0.001(7)
O25	0.032(7)	0.028(8)	0.025(8)	0.004(6)	0.001(6)	0.002(6)
O26	0.043(8)	0.009(6)	0.035(8)	−0.005(6)	−0.019(6)	−0.002(6)
O27	0.035(8)	0.024(8)	0.041(10)	−0.001(6)	−0.018(7)	0.011(7)
O28	0.045(8)	0.040(9)	0.029(9)	−0.002(7)	0.008(7)	−0.027(7)
O29	0.034(8)	0.049(10)	0.032(9)	−0.015(7)	−0.009(7)	−0.002(7)
O30	0.037(8)	0.045(9)	0.016(8)	0.003(7)	0.006(6)	−0.020(7)
O31	0.035(8)	0.028(8)	0.040(9)	−0.012(6)	−0.014(7)	0.003(7)
O32	0.014(6)	0.040(9)	0.043(9)	0.006(6)	−0.001(6)	−0.013(7)
O33	0.061(10)	0.020(7)	0.018(8)	−0.002(7)	−0.015(7)	−0.001(6)
O34	0.026(7)	0.038(9)	0.066(11)	−0.008(7)	−0.029(7)	−0.013(8)
O35	0.039(9)	0.079(13)	0.031(9)	0.032(8)	−0.008(7)	−0.026(9)
O36	0.031(7)	0.024(8)	0.042(9)	−0.007(6)	−0.015(6)	−0.010(7)
O37	0.056(9)	0.016(7)	0.025(8)	0.001(6)	−0.014(7)	−0.005(6)
O38	0.042(8)	0.010(7)	0.049(10)	0.006(6)	−0.035(7)	−0.001(6)
O39	0.043(8)	0.035(9)	0.034(9)	0.018(7)	−0.022(7)	−0.013(7)
O40	0.051(9)	0.024(8)	0.041(9)	0.001(7)	−0.016(7)	−0.017((7)
O41	0.035(8)	0.038(9)	0.033(9)	−0.017(7)	−0.015(6)	−0.015(7)
O42	0.026(7)	0.023(7)	0.019(7)	0.005(6)	−0.005(5)	−0.005(6)

significant interatomic metal-oxygen distances, uranyl angles and valence bonds calculated using Brese and O'Keeffe data [57] with $b=0.37$ Å except for U–O bonds where the coordination independent parameters ($R_{ij}=2.051$ Å, $b=0.519$ Å) were taken from Burns et al. [58].

3. Crystal structure description of $Cs_6[(UO_2)_2(MoO_4)_3(MoO_5)]$ and discussion

The structure of $Cs_6[(UO_2)_2(MoO_4)_3(MoO_5)]$ contains four symmetrically independent U^{6+} cations. Each uranium atom is

Table 5

Interatomic distances (Å), valence bond and uranyl angles (deg.) in $Cs_6(UO_2)_2(MoO_4)_3(MoO_5)$.

Atom	Distance	s_{ij}	Atom	Distance	s_{ij}
U1–O2	1.803(12)	1.613	U2–O1	1.805(13)	1.606
U1–O8	1.806(13)	1.603	U2–O13	1.811(14)	1.588
U1–O6	2.179(12)	0.781	U2–O12[ii]	2.195(13)	0.756
U1–O24	2.378(15)	0.534	U2–O27[ii]	2.345(13)	0.566
U1–O42	2.398(11)	0.512	U2–O42[ii]	2.395(12)	0.515
U1–O21[i]	2.415(15)	0.497	U2–O25	2.394(12)	0.516
U1–O14	2.449(12)	0.464	U2–O20[iii]	2.443(14)	0.470
Σs_{ij}		**6.004**	Σs_{ij}		**6.017**
U3–O5	1.791(12)	1.650	U4–O9	1.798(13)	1.628
U3–O10	1.806(13)	1.600	U4–O4	1.812(13)	1.585
U3–O23	2.182(13)	0.777	U4–O7[vi]	2.194(14)	0.761
U3–O36	2.346(15)	0.566	U4–O26[vi]	2.381(12)	0.528
U3–O15	2.376(11)	0.535	U4–O38[iv]	2.389(16)	0.520
U3–O34[iv]	2.410(15)	0.501	U4–O15[vi]	2.403(12)	0.508
U3–O22[v]	2.451(11)	0.464	U4–O33	2.406(12)	0.505
Σs_{ij}		**6.093**	Σs_{ij}		**6.035**
Mo1–O31	1.710(13)	1.703	Mo2–O40	1.731(16)	1.609
Mo1–O35	1.715(16)	1.676	Mo2–O32	1.745(12)	1.549
Mo1–O24	1.759(15)	1.488	Mo2–O36	1.749(14)	1.533
Mo1–O27	1.773(13)	1.436	Mo2–O26	1.756(11)	1.504
Σs_{ij}		**6.303**	Σs_{ij}		**6.195**
Mo3–O11	1.722(12)	1.644	Mo4–O29	1.725(13)	1.635
Mo3–O30	1.740(14)	1.575	Mo4–O39	1.735(15)	1.592
Mo3–O14	1.768(12)	1.456	Mo4–O7	1.884(12)	1.064
Mo3–O34	1.773(17)	1.436	Mo4–O23	1.899(11)	1.022
Σs_{ij}		**6.111**	Mo4–O15	2.010(13)	0.757
			Σs_{ij}		**6.07**
Mo5–O37	1.739(16)	1.579	Mo6–O3	1.728(12)	1.627
Mo5–O19	1.747(11)	1.537	Mo6–O16	1.742(16)	1.562
Mo5–O12	1.867(12)	1.114	Mo6–O22	1.763(10)	1.472
Mo5–O6	1.899(11)	1.019	Mo6–O21	1.775(14)	1.425
Mo5–O42	2.056(13)	0.669	Σs_{ij}		**6.086**
Σs_{ij}		**5.918**			
Mo7–O17	1.714(13)	1.685	Mo8–O28	1.725(14)	1.635
Mo7–O18	1.743(15)	1.562	Mo8–O41	1.749(17)	1.533
Mo7–O20	1.778(14)	1.421	Mo8–O38	1.764(14)	1.476
Mo7–O33	1.796(13)	1.35	Mo8–O25	1.766(12)	1.464
Σs_{ij}		**6.018**	Σs_{ij}		**6.108**
Cs1–O17[vii]	3.047(13)	0.182	Cs2–O1[ii]	2.968(11)	0.226
Cs1–O30	3.110(12)	0.154	Cs2–O2	3.005(12)	0.204
Cs1–O8	3.134(15)	0.144	Cs2–O26[vi]	3.055(16)	0.179
Cs1–O8[ii]	3.141(12)	0.141	Cs2–O38[iv]	3.088(13)	0.163
Cs1–O35	3.143(15)	0.141	Cs2–O3	3.127(13)	0.147
Cs1–O13	3.193(12)	0.123	Cs2–O40[vi]	3.223(13)	0.113
Cs1–O19[ii]	3.448(14)	0.062	Cs2–O41[iv]	3.278(13)	0.098
Cs1–O35[ii]	3.456(15)	0.060	Cs2–O16	3.396(12)	0.071
Cs1–O42[ii]	3.498(13)	0.054	Σs_{ij}		**1.201**
Σs_{ij}		**1.061**			
Cs3–O11[v]	2.982(13)	0.218	Cs4–O29[viii]	2.979(14)	0.219
Cs3–O39[vi]	3.054(14)	0.179	Cs4–O39	3.067(13)	0.173
Cs3–O7[vi]	3.072(13)	0.170	Cs4–O23	3.090(13)	0.162
Cs3–O4[vi]	3.183(12)	0.126	Cs4–O28[iv]	3.121(17)	0.149
Cs3–O18	3.181(14)	0.126	Cs4–O30[iv]	3.150(13)	0.138
Cs3–O4	3.245(15)	0.106	Cs4–O18	3.190(13)	0.123
Cs3–O5	3.260(13)	0.102	Cs4–O5	3.270(15)	0.099
Σs_{ij}		**1.027**	Σs_{ij}		**1.063**
Cs5–O31[i]	2.888(12)	0.281	Cs6–O12[iii]	3.042(13)	0.185
Cs5–O13	3.076(16)	0.168	Cs6–O19[ix]	3.092(13)	0.161
Cs5–O18[iii]	3.094(13)	0.161	Cs6–O37[iii]	3.222(14)	0.114
Cs5–O3[i]	3.105(15)	0.156	Cs6–O1[x]	3.232(13)	0.111
Cs5–O30	3.107(13)	0.154	Cs6–O33[iii]	3.266(15)	0.101
Cs5–O35[ii]	3.126(15)	0.148	Cs6–O41[x]	3.324(13)	0.086
Cs5–O5[iii]	3.496(12)	0.054	Cs6–O25[x]	3.341(16)	0.082
Σs_{ij}		**1.122**	Cs6–O25	3.394(12)	0.071
			Cs6–O20[iii]	3.430(14)	0.065
			Σs_{ij}		**0.976**
Cs7–O6	2.908(14)	0.265	Cs8–O19[ii]	3.050(12)	0.181
Cs7–O9	2.991(12)	0.212	Cs8–O7[xi]	3.145(11)	0.139
Cs7–O37	3.067(14)	0.172	Cs8–O29[xi]	3.154(14)	0.136
Cs7–O10[vi]	3.070(11)	0.172	Cs8–O17[vii]	3.281(14)	0.097

Table 5 (*continued*)

Atom	Distance	s_{ij}	Atom	Distance	s_{ij}
Cs7–O16[i]	3.129(12)	*0.146*	Cs8–O28	3.283(14)	*0.096*
Cs7–O28[v]	3.134(16)	*0.144*	Cs8–O12[ii]	3.357(12)	*0.079*
Cs7––O41[v]	3.326(12)	*0.085*	Cs8–O30	3.465(17)	*0.059*
Cs7–O21[i]	3.388(14)	*0.072*	Cs8–O33[vii]	3.495(15)	*0.054*
Σs_{ij}		**1.268**	Cs8–O9[vii]	3.525(13)	*0.050*
			Cs8–O13	3.585(13)	*0.043*
			Σs_{ij}		**0.934**
Cs9–O39[viii]	3.107(16)	*0.155*	Cs10–O24	3.096(12)	*0.160*
Cs9–O23	3.155(11)	*0.136*	Cs10–O3	3.120(12)	*0.150*
Cs9–O32[xii]	3.192(13)	*0.123*	Cs10–O32[vii]	3.133(14)	*0.144*
Cs9–O29	3.279(14)	*0.097*	Cs10–O11	3.236(12)	*0.109*
Cs9–O11[iv]	3.301(14)	*0.091*	Cs10–O40[vi]	3.254(16)	*0.104*
Cs9–O28[xi]	3.307(13)	*0.090*	Cs10–O5[vii]	3.260(13)	*0.102*
Cs9–O4[viii]	3.382(13)	*0.074*	Cs10–O14	3.272(11)	*0.099*
Cs9–O34[iv]	3.432(13)	*0.064*	Cs10–O18[vii]	3.507(17)	*0.052*
Cs9–O10	3.434(14)	*0.064*	Cs10–O36[vii]	3.633(13)	*0.037*
Cs9–O16[viii]	3.552(16)	*0.047*	Cs10–O31	3.674(15)	*0.034*
Cs9–O26[xii]	3.667(13)	*0.034*	**Σs_{ij}**		**0.991**
Σs_{ij}		**0.975**			
Cs11–O19[ii]	3.084(12)	*0.165*	Cs12–O32[vii]	2.950(13)	*0.237*
Cs11–O27[xiii]	3.096(12)	*0.160*	Cs12–O22[xi]	3.089(14)	*0.163*
Cs11–O6[ii]	3.103(11)	*0.157*	Cs12–O36[vi]	3.161(14)	*0.134*
Cs11–O20[vii]	3.143(12)	*0.141*	Cs12–O10[vi]	3.279(15)	*0.097*
Cs11–O35	3.256(19)	*0.104*	Cs12–O34	3.305(16)	*0.090*
Cs11–O3[xiii]	3.382(13)	*0.074*	Cs12–O21[i]	3.348(13)	*0.081*
Cs11–O8[ii]	3.432(13)	*0.064*	Cs12–O14	3.382(14)	*0.073*
Cs11–O41[xiv]	3.471(17)	*0.058*	Cs12–O22[i]	3.439(13)	*0.063*
Cs11–O17[vii]	3.595(14)	*0.042*	Cs12–O2	3.461(12)	*0.060*
Σs_{ij}		**0.965**	Cs12–O40[vi]	3.582(14)	*0.043*
			Σs_{ij}		**1.041**
Uranyl angles (deg.)					
O2–U1–O8	***175.5(6)***		***O1–U2–O13***	***177.3(6)***	
O5–U3–O10	***175.5(6)***		***O9–U4–O4***	***177.5(6)***	

Symmetry codes: (**i**) $1+x, y, z$; (**ii**) $1-x, -y, -z$; (**iii**) $1+x, -1+y, z$; (**iv**) $-1+x, 1+y, z$; (**v**) $x, 1+y, z$; (**vi**) $-x, 1-y, 1-z$; (**vii**) $x, -1+y, z$; (**viii**) $-1-x, 1-y, 1-z$; (**ix**) $2-x, -y, -z$; (**x**) $2-x, -1-y, -z$; (**xi**) $-x, -y, 1-z$; (**xii**) $-1+x, y, z$; (**xiii**) $-x, -y, -z$; (**xiv**) $1-x, -1-y, -z$.

strongly bonded to two oxygen atoms, forming an approximately linear uranyl ion $[O=U=O]^{2+}$, with average bond-lengths $\langle U=O \rangle$ of 1.804(12), 1.808(13), 1.794(12) and 1.805(13) Å with uranyl angles $[O(2)=U(1)=O(8)]=175.5(5)°$; $[O(1)=U(2)=O(13)]=177.3(6)°$; $[O(5)=U(3)=O(10)]=175.5(5)°$; $[O(9)=U(4)=O(4)]=177.5(6)°$, for U(1), U(2), U(3) and U(4), respectively. Each uranyl ion is coordinated by five additional oxygen atoms in his equatorial plane, to form a pentagonal bipyramid $(UO_2)O_5$, with mean $\langle U-O_{eq} \rangle$ equatorial bond-lengths of 2.364(12), 2.354(12), 2.353(13) and 2.355(13) Å, for U(1), U(2), U(3) and U(4), respectively. The calculated average values of uranium–oxygen distances are in excellent agreement with the average bond lengths of $\langle U=O \rangle = 1.79(4)$ and $\langle U-O_{eq} \rangle = 2.37(9)$ Å determined from numerous well refined structures by Burns et al. [58] for uranyl ions in pentagonal bipyramidal coordination. The valence bond sums are in the range of 6.004–6.093 v.u., in agreement with the expected ($+VI$) valence of uranium.

There are eight symmetrically independent Mo^{6+} cations in the structure. The six molybdenum cations Mo(1), Mo(2), Mo(3), Mo(6), Mo(7) and Mo(8) are coordinated by four oxygen atoms located at the vertices of tetrahedra, with Mo–O bond lengths in the range of 1.71(1)–1.79(1) Å. Each MoO_4 tetrahedron contains two slightly shorter Mo–O distances concerning non-linked oxygen atoms and two longer Mo–O bond-lengths relative to the oxygen atoms shared with $(UO_2)O_5$ pentagonal bipyramids. The $\langle Mo-O \rangle$ distances of these tetrahedra range between 1.74(1) and 1.76(1) Å, in good agreement with values in MoO_4 tetrahedra-containing uranyl molybdates [23,38,39,44]. The valence bond sums for these molybdenum atoms are in the range of 6.018–6.303. The Mo(4) and Mo(5) molybdenum

atoms are surrounded by five oxygen atoms to form a strongly distorted MoO_5 environment. Each distorted MoO_5 polyhedron consists of four Mo–O distances in the range of 1.72(1)–1.90(1) Å and one Mo–O bond length of 2.01(1) and 2.06(1) Å for Mo(4) and Mo(5), respectively. In this coordination, bond valence sums calculation provide 6.07 and 5.92 v.u. values for Mo(4) and Mo(5), respectively. The long Mo–O distances of 2.01(1) and 2.06(1) Å correspond to 0.757 and 0.669 v.u. for Mo(4)–O(15) and Mo(5)–O(42), respectively, exclusion of these bonds would result in serious deficiencies in the bond valence sums for Mo(4), Mo(5), O(15) and O(42) atoms, (see Table 5). Similar coordination of Mo^{6+} cation has been already observed in the structure of two other compounds containing uranyl ion : in $Cs_4(UO_2)_3O(MoO_4)_2(MoO_5)$, where there are four Mo–O distances in the range of 1.71(2)–1.87(2) Å, and one at 2.27(2) Å [24], and in the structure of deloryite $Cu_4(UO_2)(Mo_2O_8)(OH)_6$ with four short Mo–O distances ranged from 1.77(2) to 1.88(2) Å and a large bond length of 2.58(2) Å [59]. This distorted coordination was also found for W^{6+} in the structure of $Rb_6[(UO_2)_2(WO_4)_4]$, where two tungsten atoms are surrounded by five oxygen atoms to form distorted trigonal bipyramids, with a fifth W–O distance of 2.03 (2) and 2.45(3) Å [60].

The structure contains also 12 symmetrically independent Cs^+ cations surrounded by seven to nine oxygen atoms in the range of 2.89(1)–3.67(1) Å, to form complex polyhedra and giving valence bond sums between 0.934 and 1.268 v.u.

By sharing equatorial oxygen atoms O(42) and O(15), both bipyramid couples $[U(1)O_7 U(2)O_7]$ and $[U(3)O_7 U(4)O_7]$ generate two similar dimers $[U(1)O_6OU(2)O_6]^{14-}$ and $[U(4)O_6OU(3)O_6]^{14-}$, respectively. Inside each dimer $[U_2O_{13}]^{14-}$, the link between the
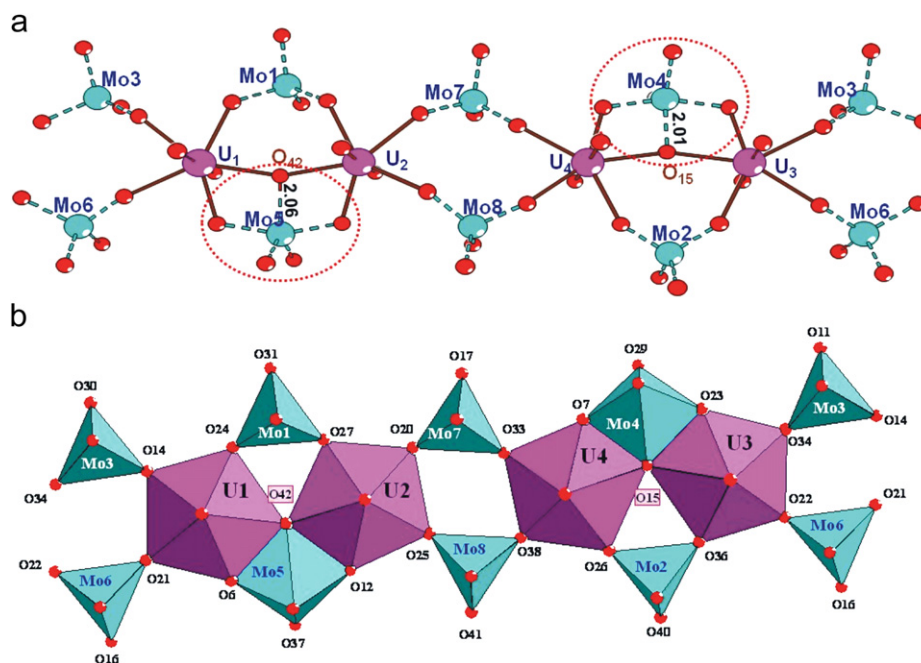
Fig. 2. The $\frac{1}{\infty}[(UO_2)_2(MoO_4)_3(MoO_5)]^{6-}$ infinite uranyl molybdate ribbons in the structure of $Cs_6[(UO_2)_2(MoO_4)_3(MoO_5)]$, (a) ball-and-stick representation and (b) polyhedral representation.

two UO_7 polyhedra is reinforced on one side by a MoO_4 tetrahedron and on another side by a MoO_5 square pyramid, to form an uranomolybdate entity $[U_2O_{13}Mo_2O_4]^{10-}$. These $[U_2O_{13}Mo_2O_4]^{10-}$ units are connected by sharing vertices with two MoO_4 tetrahedra, to form infinite ribbon $\frac{1}{\infty}[(UO_2)_2(MoO_4)_3(MoO_5)]^{6-}$ parallel to the [1 $\bar{1}$ 2] direction, Fig. 2. The infinite ribbons are associated in pseudo-layers, linked to each other by alkaline cations Cs^+, which insure the crystal structure cohesion, Fig. 3.

In the $A_6U_2Mo_4O_{21}$ compounds with $A=$Na, K and Rb, all Mo^{6+} cations are in tetrahedral MoO_4 environment to give the following developed formula $A_6[(UO_2)_2O(MoO_4)_4]$. For caesium compound, two of the eight molybdenum sites, Mo(4) and Mo(5), are coordinated with a fifth oxygen atom (O_{sh}), which is common to both uranium atoms of each U_2O_{13} dimer ,U(3)U(4)O_{13} and U(1)U(2)O_{13}. They adopt a square pyramidal MoO_5 coordination to give a different developed formulae $Cs_6[(UO_2)_2(MoO_4)_3(MoO_5)]$, Fig. 2. The fivefold coordination of the Mo atoms is realized by the formation of long Mo–O bonds with the O_{sh} atoms bridging between two U centres in the $[O_4(UO_2)O_{sh}(UO_2)O_4]$ dimmers. It is noteworthy that the arrangement of the longer Mo–O_{sh} bonds is asymmetrical relative to the chain extension.

While the Mo–O_{sh} and U–O_{sh} distances slightly and regularly decrease and increase respectively from Na to Rb compounds, the formation of square pyramidal environments for Mo(4) and Mo(5) atoms in the Cs compound is accompanied by a large variation of these distances. As a consequence, the intradimer U–U largely increases (Table 6). As can be seen from Fig. 2 the direction of the Mo(5)–O(42) bond is antiparallel to the direction of the Mo(4)–O(15) bond, i.e. the fivefold coordinated Mo atoms are located on different sides of the dimers relative to the chain extension. The identity period of the chain in the Cs compound is doubled compared to the chain in the Rb compound, and quadrupled compared to Na and K crystal structures.

The uranyl molybdate chains differ also by the relative orientation of molybdenum polyhedra. In the four compounds the molybdenum polyhedra on one side of a chain all point in the same direction, while in the compounds with the smallest ions
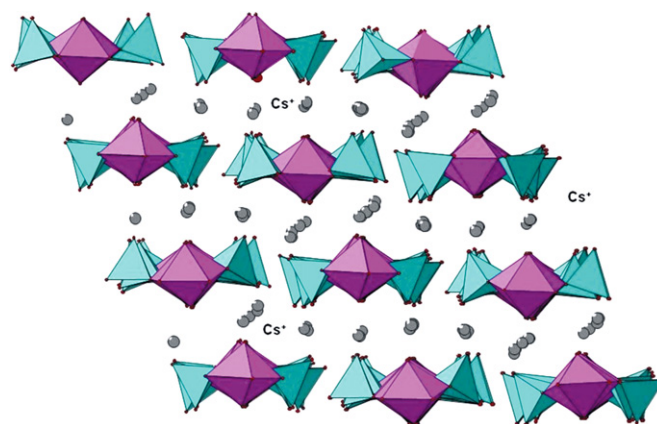

Fig. 3. Polyhedral representation of the structure of $Cs_6[(UO_2)_2(MoO_4)_3(MoO_5)]$, showing the stacking of infinite uranyl molybdate ribbons to form pseudo-layers, with interleaved Cs^+ ions.

Table 6
Evolution of average distances $\langle Mo–O_{sh}\rangle$ and $\langle U–O_{sh}\rangle$ (Å) in the $A_6(UO_2)_2(MoO_4)_3(MoO_5)$ structures ($A=$Na, K, Rb, Cs).

	Na	**K**	**Rb**	**Cs**	
Mo–O_{sh} (Å)	3.08(1)	2.99(3)	2.73(1)	2.06(1)	2.01(1)
Mo–O_{sh} (Å)	3.08(1)	2.99(3)	3.40(1)	3.44(1)	3.65(1)
U–O_{sh} (Å)	2.12(1)	2.16(3)	2.19(7)	2.38(1)	2.40(1)
			2.17(7)	2.40(1)	2.40(1)
U –U^a (Å)	4.232(3)	4.312(6)	4.267(7)	4.664(6)	4.705(6)
U–O_{sh}–U (°)	180	180	156.4(4)	154.9(5)	158.0(5)
U–U^b (Å)	6.512(4)	6.711(6)	6.679(10)	6.661(9)	6.735(9)

^{a} Intradimer U–U distance.
^{b} interdimer U–U distance.

(Na and K), the MoO_4 tetrahedra on both sides of a chain point in opposite directions, in Rb and Cs compounds they point in the same direction but in opposite direction for two adjacent chains
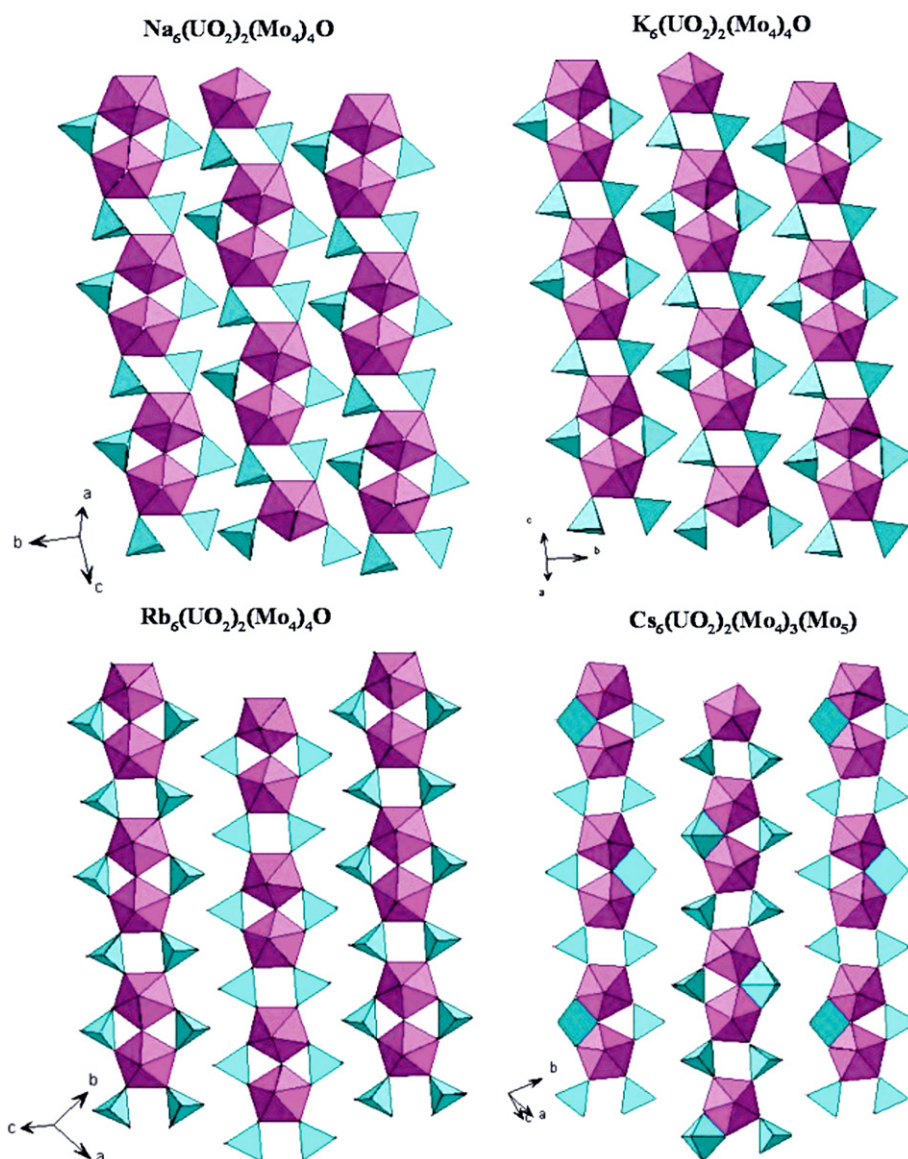
Fig. 4. Comparison of $^{1}_{\infty}[U_2Mo_4O_{21}]^{6-}$ infinite ribbons observed in the structures of $A_6U_2Mo_4O_{21}$ (A=Na, K, Rb, Cs).

(Fig. 4) leading to corrugated and linear chains, respectively, and for all compounds to pseudo-layers, linked together by A^+ alkaline cations, Fig. 5. These differences explain the unexpected unit cell volume variation, while the unit cell volume decrease from Na to K and from Rb to Cs, the unit cell volumes of K and Rb compounds are almost equal.

4. Thermal analysis, electrical conductivity and infrared spectroscopy results

Differential Thermal Analysis study of each sample showed an endothermic peak due to a non-congruent melting point, with decomposition temperatures ranging between 540 and 610 °C from Cs to Na containing compound. The powder X-ray diffraction analysis of residue, after each DTA measurement, confirmed the product as a mixture of, $(UO_2)MoO_4$, A_2MoO_4 and A_2O (A=Na, K, Rb, Cs). The decomposition sequence of $A_6U_2Mo_4O_{21}$ is shown below

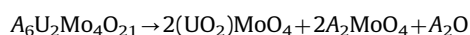$$A_6U_2Mo_4O_{21} \rightarrow 2(UO_2)MoO_4 + 2A_2MoO_4 + A_2O$$

Fig. 6 shows the temperature dependence of the conductivity for the four compounds. The observed linear variation of log σ versus $1/T$ shows that the ionic conductivity obeys to the Arrhenius law over the investigated temperature range, with high activation energy values of about 0.87; 0.88, 0.97 and 1.08 eV for Na^+, K^+, Rb^+ and Cs^+, respectively. The low conductivity and high activation energy observed in these compounds may be explained by the rigidity of their environment in the spaces located between chains and by their coordination by oxygen atoms not involved in the chain formation. As expected from the ionic radius increase, the conductivity decreases from Na to Cs.

The infrared spectra of $A_6U_2Mo_4O_{21}$ family (A=Na, K, Rb, and Cs), given in Fig. 7, are characterized by the vibrations of uranyl UO_2^{2+}, equatorial (secondary) U–O_{eq} bonds in pentagonal environment and MoO_n polyhedra (n=4 tetrahedra for Na, K, Rb, Cs and n=5 square pyramids only for Cs). For all compounds, the vibration modes in the frequency domain of 933–903 cm^{-1}, may be assigned to the asymmetric stretching vibration ν_3 of uranyl ions UO_2^{2+}. Two vibrations were observed for Na compound (933, 903 cm^{-1}), and only one vibration in the case of the last three
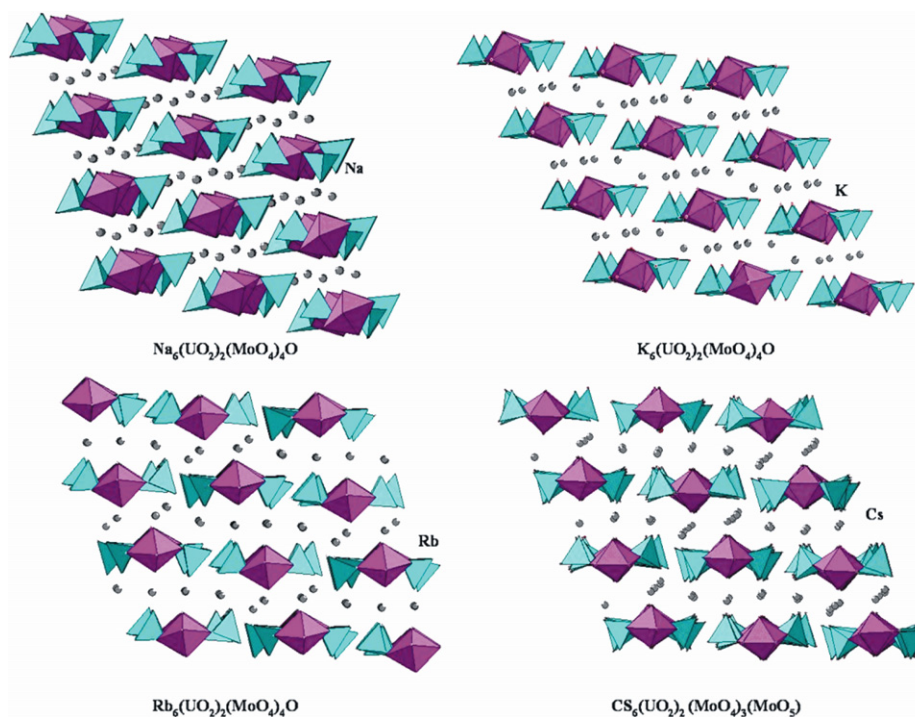
Fig. 5. Comparison of the crystal structure arrangements in the $A_6U_2Mo_4O_{21}$ (A=Na, K, Rb, Cs) compounds.
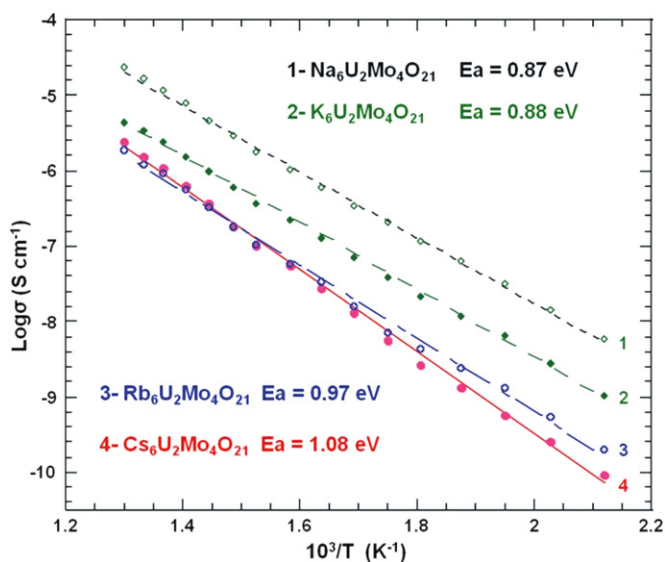

Fig. 6. Temperature dependence of ionic conductivity for $A_6U_2Mo_4O_{21}$ (A=Na, K, Rb, Cs) compounds.

other compounds, with bands at about 920, 918 and 925 cm^{-1} for K, Rb and Cs, respectively. The localized bands at 868 (Na), 847 (K), 872 (Rb), 872–848 (Cs) are assigned to the symmetric stretching vibration ν_1 UO$_2^{2+}$. The lower bands observed in the range of 518–582 cm^{-1} may be assigned to U–O$_{eq}$ vibrations between uranium and equatorial oxygen atoms. The assignment the frequency vibrations molybdenum MoO$_n$ polyhedra (n=4 tetrahedra or 5 square pyramids), are also given in Table 7.

For Cs$_6$[(UO$_2$)$_2$(MoO$_4$)$_3$(MoO$_5$)] compound, the spectrum shows two strong bands at about 925 and 848 cm^{-1}, which have been attributed to asymmetrical and symmetrical UO$_2^{2+}$ uranyl stretching vibrations ν_3 and ν_1, respectively. These two vibrations are in good agreement with the mathematical model suggested by Bagnall and Wakerley [61] to determine the value of ν_1 from
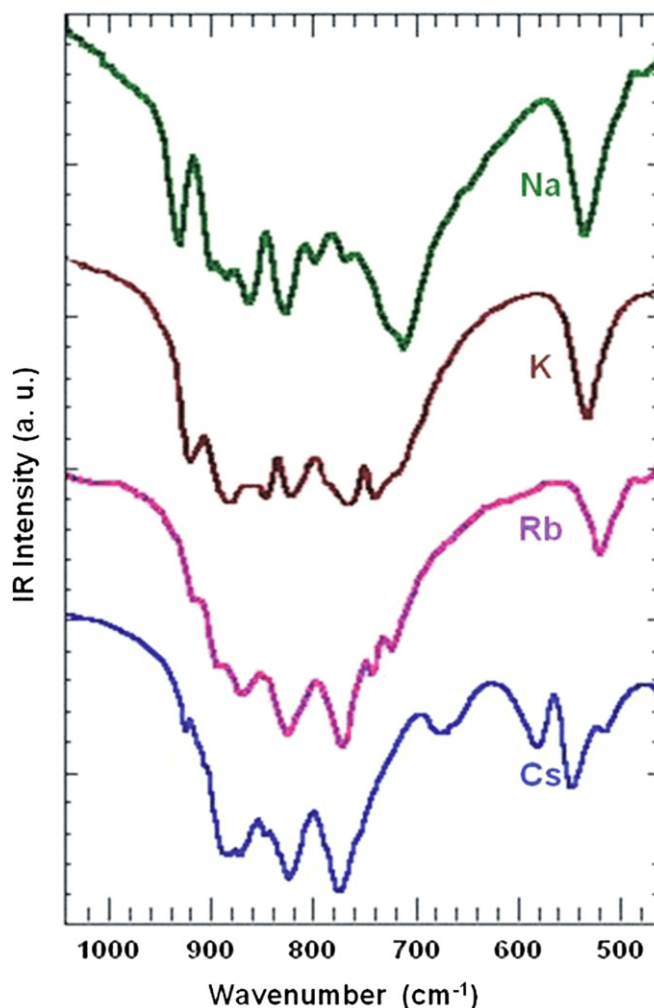

Fig. 7. Infrared absorption spectra of $A_6U_2Mo_4O_{21}$ compounds (A=Na, K, Rb, Cs).

Table 7
Infrared spectrum of $A_6U_2Mo_4O_{21}$ compounds (A=Na, K, Rb and Cs).

	Vibrational mode v (cm^{-1})			
	v_3 $(UO_2)^{2+}$	v_1 $(UO_2)^{2+}$	v U–O$_{eq}$	v MoO$_4$ and v MoO$_5$
$Na_6U_2Mo_4O_{21}$	933–903	868	540	833–891–714–771–802
$K_6U_2Mo_4O_{21}$	920	847	534	822–883–741–768
$Rb_6U_2Mo_4O_{21}$	918	872	521	829–895–725–744–775
$Cs_6U_2Mo_4O_{21}$	925	872–848	518–548–582	825–885–676–776

the one of v_3, given by the following expression:

$$v_1 = 0.912 \quad v_3 - 1.04 (\text{cm}^{-1}).$$

Thus, the application of Veal et al.'s [62] empirical equation relating bond length ($\mathbf{d_{U-O}}$) to the asymmetric stretching vibration v_3 (925 cm^{-1}) for uranyl groups

$$d_{U-O} = 81.2 v_3^{-2/3} + 0.895$$

leads to the predicted uranyl bond length of 1.1.801 Å, in good agreement with the average value obtained from X-ray structure results, $\langle U-O \rangle = 1.804(6)$ Å.

5. Conclusion

A new compound of the $A_6U_2Mo_4O_{21}$ series has been prepared for A=Cs. Its structure is, as the other compounds previously reported for A=Na, K, Rb, characterized by infinite uranyl molybdate chains. However some differences appear within the chains and in the chains arrangement illustrating the key role of the ionic radius of the monovalent cation, in particular with the formation, of penta-coordinated molybdenum atoms with Cs. Study of such compounds involving two monovalent cations and divalent cations are planned with the aim to precise this role and to obtain other geometric isomers of the uranyl molybdate chains.

References

[1] P.C. Burns, R.J. Finch, Reviews in Mineralogy. Uranium: Mineralogy, Geochemistry and the Environment, vol. 38, Mineralogical Society of America, Washington, DC, 1999.
[2] S.V. Krivovichev, P.C. Burns, I.G. Tananaev (Eds.), Structural Chemistry of Inorganic Actinide Compounds, Elsevier, Amsterdam, 2007
[3] R.J. Finch, R.C. Ewing, J. Nucl. Mater. 190 (1992) 133.
[4] E.C. Pearcy, J.D. Prikryl, W.M. Murphy, B.W. Leslie, Appl. Geochem. 9 (1994) 713.
[5] D.J. Wronkiewicz, J.K. Bates, T.J. Gerding, E. Veleckis, B.S. Tani, J. Nucl. Mater. 190 (1992) 107.
[6] D.J. Wronkiewicz, J.K. Bates, S.F. Wolf, E.C. Buck, J. Nucl. Mater. 238 (1996) 431.
[7] R.J. Finch, E.C. Buck, P.A. Finn, J.K. Bates, Mater. Res. Soc. Symp. Proc. 556 (1996) 431.
[8] P.A. Finn, S.F. Wolf, R.A. Leonard, R.J. Finch, E.C. Buck, in : Proceedings of the Seventh International Conference on the Chemistry an Migration Behaviour of Actinides and Fission Products in the Geosphere, Incline Village, Lake Tahoe, NV, USA, September 26–October 1, 1999, Abstract, vol. 7 (1999) 17.
[9] P.A. Finn, J.C. Hoh, S.F. Wolf, S.A. Slater, J.K. Bates, Radiochim. Acta 74 (1996) 65.
[10] E.C. Buck, D.J. Wronkiewicz, P.A. Finn, J.K. Bates, J. Nucl. Mater. 249 (1997) 70.
[11] R.J. Finch, J. Suksi, K. Rasilainen, R.C. Ewing, Mater. Res. Soc. Symp. Proc. 412 (1996) 823.
[12] E.C. Buck, R.J. Finch, P.A. Finn, J.K. Bates, Mater. Res. Soc. Symp. Proc. 506 (1998) 87.
[13] P.C. Burns, J. Nucl. Mater. 265 (1999) 218.
[14] P.C. Burns, R.J. Finch, F.C. Hawthorne, M.L. Miller, R.C. Ewing, J. Nucl. Mater. 249 (1997) 199.
[15] P.C. Burns, F.C. Hill, Can. Mineral. 38 (2000) 175.
[16] P.C. Burns, R.A. Olson, R.J. Finch, J.M. Hanchar, Y.J. Thibault, J. Nucl. Mater. 278 (2000) 290.
[17] P.C. Burns, R.C. Ewing, M.L. Miller, J. Nucl. Mater. 245 (1997) 1.
[18] P.C. Burns, Can. Mineral. 43 (2005) 1839.
[19] M. Ross, H.T. Evans, J. Inorg. Nucl. Chem. 15 (1960) 338.
[20] T.I. Krasovskaya, Yu.A. Polyakov, I.A. Rozanov, Izv. Akad. Nauk SSSR, Neorg. Mater 16 (1980) 1824.
[21] V.N. Serezhkin, E.E. Tatarinova, L.B. Serezhkina, Zh. Neorg. Khim. 32 (1987) 227.
[22] R.K. Rastsvetaeva, A.V. Barinova, A.M. Fedoseev, N.A. Budantseva, Yu.V. Nikolaev, Dokl. Chem. 365 (1999) 52.
[23] S.V. Krivovichev, P.C. Burns, Can. Mineral. 39 (2001) 207.
[24] S.V. Krivovichev, P.C. Burns, Can. Mineral. 40 (2002) 201.
[25] S.V. Krivovichev, C.L. Cahill, P.C. Burns, Inorg. Chem. 41 (2002) 34.
[26] S.V. Krivovichev, P.C. Burns, Can. Mineral. 43 (2005) 713.
[27] E.V. Nazarchuk, S.V. Krivovichev, S.K. Filatov, Radiochemistry 46-5 (2004) 438 Translated from Radiokhimiya 46 (2004) 405.
[28] E.V. Nazarchuk, S.V. Krivovichev, P.C. Burns, Radiochemistry 47-5 (2005) 447 Translated from Radiokhimiya 47 (2005) 408.
[29] E.V. Alekseev, S.V. Krivovichev, T. Armbruster, W. Depmeier, E.V. Suleimanov, E.V. Chuprunov, A.V. Golubev, Z. Anorg. Allg. Chem. (2007) 1979.
[30] C. Dion, A. Noël, Bull. Soc. Chim. Fr. 9-10 (1981) 371.
[31] C. Dion, A. Noël, Bull. Soc. Chim. Fr. 11–12 (1983) 257.
[32] G.G. Tabachenko, L.M. Kovba, V.P. Serzhkin, Koord. Khim. 10 (1983) 558.
[33] G.G. Sadikov, T.I. Krasovskaya, Yu.A. Polyakov, V.P. Nikolaev, Izv. Akad Nauk SSSR, Neorg. Mater 24 (1988) 109.
[34] I. Duribreux, Ph.D. Thesis, Université des Sciences et Technologies de Lille, 1997.
[35] N.L. Misra, K.L. Chawla, V. Venugopal, N.C. Jayadevan, D.D. Sood, J. Nucl. Mater. 226 (1997) 120.
[36] R.K. Rastsvetaeva, A.V. barinova, A.M. Fedoseev, N.A. Budantseva, Yu.P. Nekrasov, Dokl. Akad. Nauk. 365 (1999) 68.
[37] V.N. Krustalev, G.B. Andreev, M. Yu., A.M. Antipin, N.A. Fedosev, Bbudantseva, I.B. Shirokova, Zh. Neorg. Khim 45 (2000) 1996.
[38] S.V. Krivovichev, P.C. Burns, Can. Mineral. 39 (2001) 197.
[39] S.V. Krivovichev, P.C. Burns, J. Solid State Chem. 168 (2002) 245.
[40] S.V. Krivovichev, P.C. Burns, Inorg. Chem. 41 (2002) 4108.
[41] S.V. Krivovichev, R.J. Finch, P.C. Burns, Can. Mineral. 40 (2002) 193.
[42] S.V. Krivovichev, P.C. Burns, Solid State Sci. 3 (2003) 45.
[43] S.V. Krivovichev, C.L. Cahill, P.C. Burns, Inorg. Chem. 42 (2003) 2459.
[44] S. Obbade, S. Yagoubi, C. Dion, M. Saadi, F. Abraham, J. Solid State Chem. 174 (2003) 19.
[45] S. Yagoubi, Ph.D. Thesis, Université des Sciences et Technologies de Lille, 2004, pp. 39.
[46] S. Yagoubi, S. Obbade, C. Dion, M. Saadi, F. Abraham, Oral comm. H-34, European Symposium, "35$^{\text{ièmes}}$ Journées des Actinides", Baden-Vienne, Austria, 23–26 avril 2005.
[47] H.M. Rietveld, Acta Crystallogr. 22 (1967) 151.
[48] H.M. Rietveld, Acta Crystallogr. 25 (1992) 589.
[49] J. Rodrigez Carvajal, M.T. Fernandez Diaz, J.L. Martinez, J. Phys.: Condens. Matter 3 (1991) 3215.
[50] C. Caglioti, A. Paoletti, E.P. Ricci, Nucl. Instrum. Methods 3 (1958) 223.
[51] G. Smith, R.J. Snyder, J. Appl. Crystallogr. 12 (1979) 60.
[52] SAINT Plus Version 6.22, Bruker Analytical X-ray Systems, Madison, WI, 2001.
[53] R.H. Blessing, Acta Crystallogr. A 51 (1995) 33.
[54] G.M. Sheldrick, SHELXS-86, Program for Crystal Structure Determination, University of Göttingen, Germany, 1986.
[55] G.M. Sheldrick, "SHELXTL NT, Program Suite for solution and Refinement of Crystal Structure" version 5.1, Bruker Analytical X-ray Systems, Madison, WI, 1998.
[56] J.A. Ibers, W.C. Hamilton (Eds.), International Tables for X-Ray Crystallography, vol. IV, Kynoch Press, Birmingham, UK, 1974
[57] N.E. Brese, M. O'Keeffe, Acta Crystallogr. B 47 (1991) 192.
[58] P.C. Burns, R.C. Ewing, F.C. Hawthorne, Can. Mineral. 35 (1997) 1551.
[59] D.Yu. Pushcharovskii, R.K. Rastsvetaeva, H. Sarp, J. Alloys Compd. 226 (1996) 23.
[60] E.V. Alekseev, S.V. Krivovichev, W. Depmeier, T. Armbruster, H. Katzke, E.V. Suleimanov, E.V. Chuprunov, J. Solid State Chem. 179 (2006) 2977.
[61] K.W. Bagnall, M.W. Wakerley, J. Inorg. Nucl. Chem. 37 (1) (1975) 329.
[62] B.W. Veal, D.J. Lam, W.T. Carnall, H.R. Hestra, Phys. Rev. B (1975) 5651.